Research Square

Preprints are preliminary reports that have not undergone peer review.
They should not be considered conclusive, used to inform clinical practice,
or referenced by the media as validated information.

Implication of N-methyl-D-aspartate receptor In Homocysteine Induced Age related Macular Degeneration

Yara A. Samra
Mansoura University Faculty of Pharmacy
Dina Kira
Augusta University
Pragya Rajpurohit
Augusta University
Riyaz Mohamed
Augusta University
Leah Owen
University at Buffalo Jacobs School of Medicine and Biomedical Sciences: University at Buffalo School of Medicine and Biomedical Sciences
Akbar Shakoor
University at Buffalo Jacobs School of Medicine and Biomedical Sciences: University at Buffalo School of Medicine and Biomedical Sciences
Ivana Kim
Massachusetts Eye and Ear Infirmary
Margaret M. DeAngelis
University at Buffalo School of Medicine and Biomedical Sciences
Nader Sheibani
University of Wisconsin-Madison Molecular and Environmental Toxicology Center: University of Wisconsin-Madison School of Medicine and Public Health
Mohamed Al-Shabrawey
Augustana University
Amany Tawfik (amtawfik@augusta.edu)
Augusta University

Research

Keywords: N-methyl-D-aspartate receptor, Homocysteine, Age Related macular degeneration, Blood retinal barrier, cystathionine-β—synthase and mouse

Posted Date: May 10th, 2021

DOI: https://doi.org/10.21203/rs.3.rs-481688/v1

License: This work is licensed under a Creative Commons Attribution 4.0 International License.
Read Full License

Abstract

Background: Age related macular degeneration (AMD) is a leading cause of vision loss in old people. Elevated homocysteine (Hcy), known as Hyperhomocysteinemia (HHcy) was reported in association with AMD. We previously reported that HHcy induces AMD like features. The current study suggests activation of N-Methyl-D-aspartate receptor (NMDAR) in retinal pigment epithelium (RPE) cells as a mechanism for HHcy-induced AMD. Serum Hcy and cystathione-β-synthase enzyme (CBS) were assessed by ELISA in AMD patients. The involvement of NMDAR in Hcy's induced AMD features were evaluated 1)-*In-vitro* using ARPE-19 cells, primary RPE isolated from mice model of HHcy (CBS) and mouse choroidal endothelial cells (MCEC). 2)-*In-vivo using* wild type mice and mice deficient in RPE cells NMDAR (*$NMDAR^{R-/-}$)* with/without intravitreal injection of Hcy. Expression of retinal isolectin-B4, Ki67, HIF-1α, VEGF, NMDAR1 and albumin were assessed by immunofluorescence (IF), Western blot (WB), Optical coherence tomography (OCT), and fluorescein angiography (FA) to evaluate retinal structure, fluorescein leakage and development of choroidal neovascularization (CNV) in living mice.

Results: Serum of the neovascular AMD patients showed significant increase in Hcy and decrease in CBS levels. Moreover, Hcy significantly increased angiogenic markers; HIF-1α, VEGF and NMDAR in RPE cells and Ki67 in MCEC. Hcy-injected WT mice showed disrupted retinal morphology and development of CNV. Knocking down NMDAR in RPE improved retinal structure and CNV induction.

Conclusion: Our findings underscore the potential role for NMDAR in RPE cells in mediating Hcy-induced features of AMD and CNV induction, thus NMDAR inhibition could provide a promising therapeutic target for AMD.

Background

Age related macular degeneration (AMD) is a leading cause of vision loss in people over 60 (1) (2). The projected number of people with AMD in 2020 was 196 million, and is forecasted to increase to 288 million by 2040. In the United States alone, 11 million new cases are diagnosed per year (3). Annual costs for direct health care due to AMD in the US is $255 billion, which is ~ half the direct cost of all vision loss ($513 billion), making AMD the leading cause of visual disability in the developed world and third globally (4). The pronounced socioeconomic burden resulting from these patients, lack of productivity, high treatment costs, and diminished quality of life underscores the urgent need for a new therapy to treat AMD. Major advances have been made in the past decades in treating the wet form of AMD to target established abnormal blood vessel growth through anti-VEGF therapy. Yet current AMD therapy is still unable to prevent or cure this pathology as the majority of patients require indefinite treatment, do not regain vision, or demonstrate progression of disease despite therapies. Unless the disease is prevented, delayed, or treated effectively, affected individuals will continue to suffer and health care costs will continue to rise.

Over the last ten years elevated homocysteine (Hcy) has raised special attention in relation to AMD in several clinical studies, suggesting an association between elevated serum Hcy levels and the risk of AMD (5) (6) (7) (8). Furthermore, our work reported a direct impact of excess Hcy (known as Hyperhomocysteinemia, (HHcy) on retinal pigment epithelium (RPE) structure, barrier function and induced choroidal neovascularization (CNV) in mice (9). We also reported that HHcy increased VEGF levels in retina (10) angiogenic potential of retinal endothelial cells *in vitro* (11). Understanding the molecular mechanism by which Hcy contributes to the pathogenesis of AMD remains a critical barrier in proposing Hcy as a biomarker and/or a therapeutic target for the treatment of AMD.

The activation of N-methyl D-aspartate (NMDA) receptors has been suggested as a possible mechanism of HHcy-induced retinal ganglion cell death during diabetic retinopathy (DR) (12) (13) (14). Several studies have identified NMDAR as a receptor for Hcy in neurons (15). NMDAR is expressed in cerebral endothelium and involved in glutamate-induced damage to endothelial cell (EC) integrity by disrupting tight junctions and increasing permeability (16) (17). Therefore, the NMDAR is a rational target for therapeutic intervention in HHcy. Recently, we reported activation of retinal endothelial NMDAR by Hcy leading to breakdown of BRB and its potential role as a therapeutic target in retinal diseases associated with HHcy such as DR and AMD (18). The current study is proposing the activation of NMDAR in RPE cells as an underlying target in HHcy induced AMD pathology.

The NMDAR is well known for its involvement in brain trauma and neurodegenerative disorders (19) (20). And its expression was reported to be increased in brain microvascular ECs after Hcy treatment. Furthermore, glutamate treatment increased RPE proliferation in cultured primary rat RPE cells and this was concomitant with increased positive immunostaining for NMDAR in RPE cells, suggesting that activation of the NMDA receptor stimulates proliferation of RPE cells (21).

Retinal and choroidal neovascularization are considered as the main causes of significant visual impairment, understanding the various factors involved in this pathology is vital for development of novel managements targeting for preservation of patient vision. The current study is aiming to assess the underlying molecular mechanisms of Hcy-induced RPE dysfunction. We propose that NMDAR activation in the RPE cells by HHcy is playing a fundamental role in AMD induction and blocking NMDAR in RPE could be a novel therapeutic target for patients with AMD. We also generated mice deficient in NMDAR in the RPE cells (*$NMDAR^{R\ -/-}$)* and examined, if knocking down the NMDAR in RPE cells has the ability to prevent Hcy-induced CNV and BRB permeability in AMD.

Materials And Methods

Animals:

Mouse with deletion or inhibition of NMDAR

We generated mice deficient in the RPE cells NMDAr (*NMDAR*$^{-/-R}$) by backcrossing floxed NR1 mice with C57BL/6-Tg (BEST1-cre) 1Jdun/J mice (Jackson Lab) that express Cre recombinase under the control of the human bestrophin 1 (*BEST*) promoter to investigate the involvement of NMDAR of RPE cells in HHcy-induced features of AMD **(**Fig. 4**).** These floxed NR1 mice allow deletion of the GluN1 subunit of the N-methyl-D-aspartate receptor in Cre recombinase expressing cell. This approach is useful in studying NMDAR and its downstream signaling molecules/pathways. Mice that are homozygous for this allele are viable, fertile, and normal in size, and do not display any gross physical or behavioral abnormalities. These mice have previously been used to study the role of the NMDAR in remote memories and behavior (22, 23) and our lab also generated NMDAR$^{E-/-}$, an endothelial cell conditional knockout mice, used in studying the NMDAR1 and its downstream signaling molecules/pathways and its involvement in HHcy-induced BRB dysfunction (18).

Mouse with HHcy

Pairs of cbs$^{+/-}$ mice (B6.129P2-Cbstm1Unc/J; Jackson Laboratories, Bar Harbor, ME) were bred to establish colonies of cbs$^{+/+}$, cbs$^{+/-}$, and cbs $^{-/-}$ mice. Genotyping was performed according to the Jackson animal laboratory's protocol. Based on whether the mouse is heterozygous (*cbs*$^{+/-}$) with one *cbs* copy or homozygous (*cbs*$^{-/-}$), which has no copies of *cbs* enzyme. Therefore, the *cbs*$^{+/-}$ mice have about 4- to 7-fold increase in plasma Hcy level, range from mild to moderate retinal phenotype, normal life span and represent mild/moderate HHcy, while the *cbs*$^{-/-}$ mice have about a 30-fold increase in plasma Hcy, shows severe retinal phenotype, a short life span of ~ 3 to 5 weeks and represent severe HHcy. Cbs mice have been used as a model of HHcy in our and others' publications (9, 11, 18, 24–28).

For intravitreal injection of Hcy in mice, the procedure was the same as described in our previous publications (9, 18, 26, 29). 1 µL was used as intravitreal injection volume to avoid uncontrolled intraocular pressure increase. 10X stock solution of L-Homocysteine thiolactone hydrochloride (Sigma-Aldrich, Louis, MO) was prepared in distilled water and a working solution was prepared by diluting 1 µL of stock solution (200 mM) to 100 µL with phosphate buffer saline (PBS). To obtain 200 µM vitreal concentration of Hcy-thiolactone, 1 µL of this working solution was injected. PBS-injected control eyes showed normal retinal morphology with no apparent apoptosis within 7 days, demonstrating that the volume of the injected solution apparently did not result in significant pressure induced damage in retina.

All animals used in the current study were maintained in clear plastic cages, allowed to eat and drink ad libitum and were subjected to standard laboratory conditions (12-hour light/12-hour dark light cycles, temperature 22 to 24°C). All experimental procedures were performed according to the Public Health Service Guide for the Care and Use of Laboratory Animals (Department of Health, Education, and Welfare publication, NIH 80 – 23) and Augusta University guidelines and followed the ARVO Statement for Use of Animals in Ophthalmic and Vision Research.

Measurement of Homocysteine and Cystathionine Beta-Synthase (CBS) Enzyme Levels

The concentration of Hcy and CBS enzyme levels were assessed in the serum of neovascular and non-neovascular AMD patients compared to normal control using Hcy Enzyme Linked Immunosorbent Assay (ELISA) kit from Cell Bio Labs Inc (STA-670, San Diego, CA, USA) and CBS ELISA assay kit from My BioSource (MBS700623, San Diego, CA, USA). The patient's blood samples were provided by Dr. Margaret M. DeAngelis and Institutional Review Board (IRB) was approved by the University of Utah. The blood samples collected were allowed to clot in serum separator tubes (SST) for a minimum of 2 hours at room temperature preceding to centrifugation at 1000× g for 15 min. The serum was collected and immediately assessed according to the protocol delivered with the kit. The readings were taken at 450 nm using an ELISA plate reader. Serum samples were taken from AMD patients (3 females and 2 males; age 83 ± 6.5) and controls (4 females and 6 males; age 74 ± 9.6), all donor's ancestry is Caucasian European. Donors' comorbidities (disease and normal) include dyslipidemia and hypertension and the cause of death was myocardial infarction. Donor samples were collected, determined, managed and phenotyped as previously defined for the Utah protocol (30). The clinically derived modified Age-Related Eye Disease Study severity grading scale (AREDS 1, AREDS 2, AREDS3 (intermediate), AREDS 4a (geographic atrophy), AREDS 4b (nAMD) was used (31). This protocol was approved by the IRB (IRB 00052879) at the University of Utah and conforms to the tenets of the Declaration of Helsink.

Cell Culture:

Human retinal pigmented epithelial cell line (ARPE-19) was obtained from American Type Culture Collection (ATCC, Manassas, VA, USA). ARPE-19 at passage 6–15 was cultured in DMEM/F-12 growth medium (Thermo-Scientific, Wyman, Massachusetts) supplemented with penicillin/streptomycin 1% and fetal bovine serum (FBS) 10%. At 80–90% confluency, the cells were serum starved overnight and then treated with Hcy at (20 or 50 or 100 µM, choice of treatment doses according to our previous published work) or vehicle for 24 h. After 24 h, the supernatant and/or the cells were harvested for further analyses.

Isolation and Culture of Primary Retinal Pigment Epithelium (RPE)

Wild type, $cbs^{+/-}$, $cbs^{-/-}$ and $NMDAR^{-/-R}$ mice (~ 3 week old) were used for isolation of RPE cells as previously published (32) (27). Briefly, mouse eyes were enucleated and rinsed in 5% povidone-iodine solution, then rinsed with sterile Hank's Balanced Salt Solution (HBSS). Then connective tissues were cleared away and eyes were placed in cold RPE cell culture medium (DMEM: F12), which is supplemented with 25% fetal bovine serum, 0.1 mg/mL gentamicin, 100 U/mL penicillin, and 100 µg/mL streptomycin. After that, eyes were transferred to HBSS containing 19.5 U/mL collagenase and 38 U/mL testicular hyaluronidase and incubated at 37°C for 40 min, followed by incubation in HBSS containing 0.1% trypsin (pH 8) at 37°C for 50 min. Then eyes were placed in a new dish with RPE cell culture medium at 4°C for at least half hour. After that, eyes were dissected and isolated RPE cells were centrifuged at 1200×g for 10 min (Thermo Medilite Centrifuge, Thermo Scientific, Waltham, MA), followed by suspension and culture of RPE cells in RPE cell culture medium (DMEM: F12) at 37°C.

Isolation and Culture of Mouse Choroidal Endothelial Cells (MCEC)

MCEC were isolated and maintained as previously described (33). Briefly, eyes from 4-week-old TSP1+/+ and TSP1−/− immorto-mice were enucleated. Under a dissecting microscope in cold DMEM, the anterior eye was removed, followed by the lens, vitreous, retina and optic nerve, leaving only a tissue composed of RPE, choroid and sclera. These tissues were pooled together, rinsed with DMEM, minced into small pieces in a tissue culture dish using sterilized razor blades, and digested in 5 ml of collagenase type I (1 mg/ml in serum free DMEM, Worthington, Lakewood, NJ) for 45 min at 37°C. Following digestion, DMEM with 10% FBS was added and cells were pelleted. The cellular digests then were filtered through a double layer of sterile 40 μm nylon mesh (Sefar America Inc., Fisher Scientific, Hanover Park, IL), centrifuged at 500×g for 10 min to pellet cells, washed twice with DMEM containing 10% FBS. Then, cells were suspended in 1 ml medium (DMEM with 10% FBS), and incubated with sheep anti-rat magnetic beads pre-coated with anti-PECAM-1. After affinity binding, magnetic beads were washed six times with DMEM with 10% FBS and bound cells in endothelial cell growth medium were plated into a single well of a 24 well plate pre-coated with 2 μg/ml of human fibronectin (BD Biosciences, Bedford, MA). Endothelial cells were grown in DMEM media supplemented with 10% FBS, 2 mM L-glutamine, 2 mM sodium pyrovate, 20 mM HEPES, 1% non-essential amino acids, 100 μg/ml streptomycin, 100 U/ml penicillin, freshly added heparin at 55 U/ml (Sigma, St. Louis, MO), endothelial growth supplement 100 μg/ml (Sigma, St. Louis, MO), and murine recombinant interferon-γ (R & D, Minneapolis, MN) at 44 units/ml. Cells were maintained in 1% gelatin-coated 60 mm dishes at 33°C with 5% CO_2.

Fluorescein isothiocyanate (FITC)-dextran permeability assay

ARPE-19 cells were seeded on collagen/fibronectin coated membranes with 0.4 μm pores (Transwell; Corning Costar). FITC-dextran flux permeability assays were performed as previously described (9, 11). Briefly, cells were seeded until forming a complete confluent layer then cells were incubated in serum free media for 24 hours before Hcy treatment (20, 50, or 100 μM) (Sigma-Aldrich) for 24 hours to the upper chambers in the presence or absence of NMDAR inhibitor MK801, followed by addition of 10 μM FITC-dextran to the upper chambers. Aliquots were collected from the upper and lower chambers at 1, 3, or 6 hours then placed in a 96-well plate to measure the fluorescence intensity with a plate reader. The rate of diffusive flux (Po) FITC-dextran was calculated by the following formula (34): $Po = [(FA/\Delta t)\ VA]/\ (FLA)$. Where Po is in centimeters per second; FA is lower chamber fluorescence; FL is upper chamber fluorescence; Δt is change in time; A is the surface area of the filter (in square centimeters); and VA is the volume of the lower chamber (in cubic centimeters).

Quantitative Reverse-Transcriptase Polymerase Chain Reaction (RT-q PCR) for NMDAR1

Total RNA was extracted from ARPE-19 cells and human neuroblastoma cells using TRIzolTM Reagent (Invitrogen, Eugene, Oregon, USA). Following RNA extraction and quantification, iScript™ Synthesis kit (BioRad Laboratories, Hercules, CA) was used for reverse transcription of 2 µg of RNA. For amplification of the produced cDNA, gene specific primer for NMDAR1, absolute QPCR SYBR Green Fluorescein Mix (Thermo Scientific, Surrey, and UK) and the BioRadiCycler (BioRad, Hercules, CA) were used. 18S was used as control for normalization. The primers used were NMDAR1 (NMDAR1 human F1: 5' AAG CTG AGG GTG TGA AAC GG-3', NMDAR1 human R1: 5' GAG AGC CTG GAA ACT GGA CC-3'). Amplification parameters were as follows: 40 cycles of 95°C for 30 seconds, 60°C for 30 seconds, and 72°C for 30 seconds. Melt curve analysis was performed to confirm the purity of the end products. Comparative CT method was used to obtain fold changes in gene expression [11].

Western Blot Analysis

Western Blot analysis was used to detect NMDAR, HIF-1α and VEGF in RPE cells and albumin in mice retina. After treatment of ARPE-19 with Hcy, the media was removed and cells were lysed in RIPA buffer supplemented with 1:100 (v/v) of proteinase/phosphatase inhibitor cocktail (Thermo Scientific). Also, primary RPE and mice retina were lysed in RIPA buffer supplemented with proteinase/phosphatase inhibitor cocktail. Then cell lysates and tissue homogenate were centrifuged at 12,000 xg at 4°C for 30 min. Protein conc. was determined by BCA Protein Assay (Thermo Scientific) and equal amount of protein was boiled in Laemmli sample buffer. Then samples were subjected to gel electrophoresis on sodium dodecyl sulfate-polyacrylamide gel (SDS-PAGE) and the protein was blotted to nitrocellulose membranes, which were further blocked using 5% milk solution and then incubated with NMDAR1 (Cell signaling, Danvers, MA, USA, Ca # 5704S), NMDAR2A (Cell signaling, Danvers, MA, USA, Ca # 4205s), NMDAR2B (Cell signaling, Danvers, MA. USA. Ca # 4207s), HIF-1α (Abcam, MA, USA, Cat # ab82832), VEGF (Thermofisher, MA, USA, Cat #5-13182), Albumin (Bethyl, TX, USA), GAPDH, (Sigma-Aldrich, St. Louis, MO. USA) and β actin (Cell signaling, Danvers, MA. USA. Cat #937215). Then blots were incubated with an appropriate peroxidase-conjugated secondary antibody and visualized with the enhanced chemiluminescence (ECL) western blot detection system (Thermo Scientific). ImageJ software was used to determine the optical density of the bands.

Enzyme-Linked Immunosorbent Assay (ELISA)

An ELISA kit was used to further evaluate the effect of elevated Hcy on VEGF activation by measuring the level of VEGF in ARPE-19 treated with Hcy (20, 50 and 100 µM) for 24 h. After treatment, media was removed, followed by washing twice by PBS. Then, the cells were solubilized by using cell extraction buffer and VEGF was measured in these cell lysates using Human VEGF ELISA Kit (ab100662 ELISA Kit, Abcam, Cambridge, MA, United States). Absorbance was measured by a plate reader at 450 nm.

Immuno-fluorescent Assessment

Primary Mouse Cells and Retina NMDAR1 and angiogenic factors (HIF-1α and VEGF) were assessed in primary RPE cells, Ki67 and ZO-1 were assessed in MCEC and Isolectin-B4 in Retina. Cells were fixed in 4% paraformaldehyde for 10 min, washed with PBS, and blocked for one hour with Power Block

(BioGenex, Fremont, CA), Ca. # BS-1310-25. Then cells were incubated with anti- NMDAR1 (Cell signaling, Danvers, MA, USA, Ca # 5704S), anti-HIF-1α (Abcam, MA, USA, Cat# ab82832), anti-VEGF (Thermofisher, MA, USA, Cat #5-13182) and anti- Ki67 (Abcam, MA, USA, Cat # ab15580) for 3h at 37°C. After that, cells were washed 3 times with PBS containing 0.3% Triton-X. After last wash, cells were incubated with appropriate secondary antibodies (Alexafluor and Texas red avidin, Invitrogen, Eugene, Oregon), and cover slipped with Fluoroshield containing DAPI (Sigma-Aldrich Chemical Corp., St. Louis, MO) to label the nuclei. An Axioplan-2 fluorescent microscope (Carl Zeiss, Göttingen, Germany) equipped with a high resolution microscope (HRM) camera was used to capture images using Zeiss Axiovision digital image processing software (version 4.8). Additionally, NMDAR expression was assessed in retinal RPE flat-mounts isolated from mice injected intravitreal with Hcy (WT and *NMDAR*$^{-/-R}$ mice). RPE flat-mounts were performed per our published method (27).

NMDAR expression and isolectin-B4 (marker for blood vessel) were assessed using immunofluorescence in RPE flat-mounts and retinal frozen sections (sections were prepared from wild type and Hcy injected mice) as per our published method (11). Briefly, flat-mounts and frozen sections were fixed with 4% paraformaldehyde and blocked with Power Block, then incubated with primary antibody for 3 h at 37°C. Then washed and incubated with secondary antibody (Alexafluor and Texas red avidin, Invitrogen, Eugene, Oregon), Next, mounts and sections were cover-slipped with Fluoroshield containing DAPI (Sigma-Aldrich) to label the nuclei. An Axioplan-2 fluorescent microscope (Carl Zeiss, Göttingen, Germany) equipped with a high resolution microscope (HRM) camera was used to capture images using Zeiss Axiovision digital image processing software (version 4.8). Samples were representative to at least three mice for each IF experiment.

Optical Coherence Tomography (OCT) and Fluorescein Angiography (FA)

To evaluate fluorescein leakage and retinal structure after intravitreal injection of Hcy into wild type and *NMDAR*$^{-/-R}$ mice and to evaluate fluorescein leakage and retinal structure after 2 days from laser induction of CNV in Hcy intravitreal injected mice (wild type and *NMDAR*$^{-/-R}$), OCT and FA were performed according to our published methods with some modifications (24) (9) (18, 26). Briefly, mice were injected intravitreally with Hcy (200 μM) and OCT and FA were performed after 48 hours. For laser experiment, laser induction was performed after 5 days of Hcy injection and after 2 days from laser induction OCT and FA were performed.

The mice were anesthetized using 2% isoflurane and the eye pupils were dilated by using 1% tropicamide eye drop. Then, each mouse was placed on the imaging platform of the Phoenix Micron III retinal imaging microscope supplemented with OCT imaging device (Phoenix Research Laboratories, Pleasanton, CA, USA). Lubricant gel was applied to keep the eye moist during imaging. For FA, mice were injected with (10 to 20 μL, IP) of 10% fluorescein sodium (Apollo Ophthalmics, Newport Beach, CA, USA), followed by rapid acquisition of fluorescent images ensued for ~ 5 minutes. Fluorescein leakage manifests as indistinct vascular borders progressing to diffusely hazy fluorescence.

Laser induction using Phoenix MICRON Image-Guided Laser System

Mice were placed on placed on the imaging platform the Phoenix Micron IV retinal imaging microscope after being anesthetized and prepared as mentioned in the FA&OCT imaging. The fundus was viewed with the micron IV fundus camera, and laser photocoagulation was induced using the image-guided laser system (Micron IV, Phoenix Research Laboratories, and Pleasanton, CA). The fundus image as well as the aiming beam can be observed on the monitor screen. Four to five laser burns at equal distance from the optic nerve were induced one by one in each eye by a green Argon laser pulse with a wavelength of 532 nm, duration of 70 ms, and power levels from 250 mW to 260 mW. Successful laser burns were confirmed by the appearance of white bleep with grey outline indicating break of Bruch's Membrane. After laser photocoagulation, mice were then placed under infra-red warming lamp until they awakened.

Measuring Retinal Thickness

Spectral domain OCT with guidance of bright-field live fundus image was performed with the image-guided OCT system (Phoenix Research Labs, Pleasanton, CA) according to the manufacturer's instruction and using StreamPix 6 software version 7.2.4.2 (Phoenix Research Labs, Pleasanton, CA) to generate fundus images and OCT scans. Using the InSight software, version 2.1.7237, (Phoenix Research Labs), the borderlines between the retinal layers were defined on the OCT pictures. These borderlines were initially indicated automatically by the software they were then manually corrected by the researchers if necessary. Next, the distance (in μm) between each borderline was calculated using InSight software at 300 consecutive points throughout the borderline, and the average of these data was defined as the thickness of the respective layer (NFL + IPL, INL, OPL, ONL, outer + inner segments, RPE and Choroid).

DATA ANALYSIS

Results were conveyed as mean ± SD. Assessment of differences amongst experimental groups was performed using the two-tailed t test or one-way analysis of variance (ANOVA). When statistical differences were detected using ANOVA, Tukey's post hoc test was performed to determine which groups differed. Statistical significance was considered at a confidence level of $P < 0.05$.

Results

Measurements of Homocysteine and CBS enzyme levels

Hcy and CBS enzyme levels were assessed in the serum of AMD patients and normal donors as control. Hcy level was significantly ($P < 0.05$) increased in the serum of neovascular AMD donors compared to normal control ($p < 0.05$) (Fig. 1A). Furthermore, CBS enzyme level was significantly decreased in AREDS3 (representing intermediate AMD) and neovascular AMD patients compared to normal control ($p < 0.05$) (Fig. 1B). This data suggested elevated Hcy level and impaired Hcy clearance in AMD patients especially neovascular AMD patients.

Homocysteine promotes angiogenesis and induction of choroidal neovascularization (CNV)

To study the effect of Hcy on CNV induction, we examined the CNV in retinal frozen section and retinal flat-mounts of wild-type mice (C57-BL6) injected intravitreal with/without Hcy, Retinal section/ flat-mounts were evaluated by immunofluorescence staining for vascular marker, isolectin-B4 (red). The results showed that Hcy-injected wild type mice highly expressed isolectin-B4 and showed development of blood vessels extending from the area of the choroid to the inner retina (white arrows, Fig. 1C) compared to the control wild type mice which revealed normal retinal vascular pattern. While, the isolectin-B4 stained retinal flat-mounts collected from mice with/without intravitreal injection of Hcy were exposed to laser induction to examine the effect of Hcy on the size and extent of laser induced CNV showed that Hcy significantly increased the extent of laser-induced CNV in wild type mice (Fig. 1D). Moreover, to confirm the effect of Hcy treatment on proliferation of choroidal endothelial cells, we examined the expression of Ki67 proliferation factor in cultured mouse choroidal endothelial cells (MCEC) and results showed marked increase in Ki67 expression (green) in MCEC by Hcy treatment (Fig. 1E).

Homocysteine activates HIF-1α and VEGF in RPE cells

RPE cells are an important source of angiogenic factors in the retina. To further study the involvement of RPE in Hcy induction angiogenesis and CNV, the expression of hypoxia-inducible factor (HIF-1α) which is a common transcription factor for several angiogenic proteins (35) and its downstream regulator of angiogenesis vascular endothelial growth factor (VEGF) were evaluated in primary RPE cells isolated from wild type $cbs^{+/+}$, $cbs^{+/-}$ and $cbs^{-/-}$ mice. HIF-1α level was significantly upregulated by Hcy as shown in primary RPE isolated from $cbs^{+/-}$ and $cbs^{-/-}$ mice when was evaluated by Western blot analysis (Fig. 2A) and immunofluorescence (Fig. 2B), HIF-1α was increased in the $cbs^{+/-}$ mice RPE (represent mild/moderate HHcy) and significant increase in $cbs^{-/-}$ mice RPE (represent marked increased HHcy), which was also very evident in immunofluorescence staining (red).

VEGF level was evaluated in ARPE-19 cells treated with different concentration of Hcy (20, 50, and 100 μM) and primary RPE cells isolated from wild type $cbs^{+/+}$ and $cbs^{+/-}$ and $cbs^{-/-}$ mice. VEGF level was evaluated using Western blot analysis (Fig. 2C and 2E), ELISA (Fig. 2G) and immunofluorescence staining as shown in red (Fig. 2D). Hcy significantly increased VEGF level in both ARPE-19 cells treated Hcy and primary RPE cells isolated from mice with HHcy ($cbs^{+/-}$ and $cbs^{-/-}$). Furthermore, the activation and co-localization of both HIF-1α (green) and VEGF (red) in primary RPE cells isolated from the mice with HHcy was confirmed by immunofluorescence staining (Fig. 2F).

Homocysteine activates NMDA receptors in RPE cells

NMDAR1 expression was assessed in human RPE (ARPE-19) cell line at both gene and protein levels. The gene expression of NMDAR was assessed by RT-qPCR and human neuroblastoma cells was used as a positive control. Our results showed that NMDAR1 gene is expressed in ARPE-19 cell line (Fig. 3A). And its expression is increased by Hcy treatment in a dose dependent manner (Fig. 3B). The expression of

NMDAR was further confirmed on the protein level by assessing the expression of NMDAR1 by WB and IF analysis in ARPE-19 cells treated with/without Hcy (20, 50 and 100 μM). WB and IF analysis showed that NMDAR1 is highly expressed in ARPE-19 cell line and the expression was significantly increased by 100μM Hcy treatment (Fig. 3C and 3D) compared to ARPE-19-control. Finally, to further confirm our results, protein expression of NMDAR1 was examined in the outer retina part (has good amount of RPE cells) of the mice model of HHcy (*cbs*$^{+/-}$) compared to normal control mice retina by WB analysis (Fig. 3E) and in primary RPE cells isolated from wild type mice and *cbs*$^{+/-}$ mice by immunofluorescence. *cbs*$^{+/-}$ mice showed significant expression of NMDAR1 in the outer retina and increased activation (green) in *cbs*$^{+/-}$ RPE cells compared to primary RPE cells isolated from wild type (Fig. 3F).

Mouse with deletion/inhibition of NMDAR in Retinal Pigmented Epithelia (NMDAR $^{R-/-}$ **)**

We previously reported the involvement of endothelial NMDAR in HHcy induced BRB dysfunction (18). The current study is aiming to further study the involvement of NMDAR of RPE cells in HHcy-induced features of AMD. We generated mice deficient in the RPE cells NMDAR (*NMDR*$^{R-/-}$) mouse genotyping is shown in Fig. 4A. The deletion of NMDAR was confirmed using western blotting analysis of NMDAR1 in isolated primary RPE cells isolated from *NMDR*$^{R-/-}$ mice, which revealed significant decrease of NMDAR1 in *NMDAR*$^{R-/-}$ mouse compared to wild type (Fig. 4B). Furthermore, NMDAR deletion was further confirmed in retinal RPE flat-mount isolated from wild type and *NMDAR*$^{R-/-}$ mice 72 hours after intravitreal injection of Hcy. RPE flat-mounts revealed high expression of NMDAR in wild type mice (confirming receptors activation by Hcy) compared to the *NMDAR*$^{R-/-}$ mice flat-mounts which showed marked decrease in NMDAR activation by Hcy indicating receptors deletion/ inhibition (Fig. 4C),

Effect of NMDAR Deletion in RPE cells on Hcy-induced BRB dysfunction

We reported previously, that both pharmacological (MK801) and genetic inhibition of NMDAR in retinal endothelial cells (*NMDAR*$^{E-/-}$ mouse) were able to reduce retinal damage and restore BRB induced by HHcy both in *in-vitro* and *in-vivo(18).* After confirming the expression of NMDAR in retinal pigmented epithelial cells as well as its activation by Hcy, we wanted to examine whether blocking NMDAR in RPE cells (*NMDAR*$^{R-/-}$ mouse) will rescue the retina from Hcy-induced blood retinal barrier (BRB) disruption and choroidal neovascularization (CNV) induction. We performed two functional studies both in *in-vivo* and *in-vitro*, using Fluorescein angiography (FA) and optical coherence tomography (OCT) examination for living mice and FITC dextran leakage assay in ARPE-19 cells treated with/ without different concentrations of Hcy. FA and OCT were used to evaluate vascular leakage, retinal morphology and CNV induction living mice. Three groups of mice at age ~ 6–8 weeks old were subjected to FA and OCT evaluation (wild-type (C57-BL6) compared to wild-type and *NMDAR*$^{R-/-}$ mice after 72 hours after intravitreal injection of Hcy (200 μM). FA examination showed increased fluorescein leakage (white arrows) and disrupted retinal morphology in Hcy-injected wild type mice compared to wild type control mice suggesting decreased retinal vessel integrity and impairment of BRB by Hcy. While genetic inhibition

of NMDAR by knocking down NMDAR in RPE cells (*NMDAR*$^{R-/-}$) was able to decrease fluorescein leakage (white arrows) and restored BRB (Fig. 5A). While, OCT evaluation showed a normal appearance in wild type mice, but marked disruption at the RPE layer and CNV induction (yellow arrows) in the retinas of Hcy-injected wild type mice. While, knocking down NMDAR in RPE cells (*NMDAR*$^{R-/-}$) improved retinal structure and CNV induction (yellow arrows) after Hcy injection (Fig. 5B). Vascular leakage was confirmed by measuring the albumin leakage in the retinas after perfusion using western blotting analysis after perfusion with PBS solution and as previously described in our publications (9, 18, 24, 26). Quantification of data from western blotting showed significant increase in albumin leakage in Hcy-injected mice retina compared to non-injected mice and the albumin leakage was significantly decreased in *NMDAR*$^{R-/-}$ mice injected with Hcy, suggesting that blocking of NMDAR could restore the BRB and prevent retinal leakage induced by Hcy (Fig. 5C).

To further study the effect of inhibition of NMDAR on the permeability of RPE cells treated with/without Hcy, an *in-vitro* functional assay was performed using pharmacological inhibition of NMDAR, MK801. We investigated whether Hcy induces permeability changes to FITC dextran flux through ARPE-19 confluent monolayer. Hcy (50 and 100 μM) in the presence/absence of MK801 (25 μM) was added. Our data showed that Hcy treatment significantly increased FITC dextran leakage in RPE cells monolayer and MK801 treatment significantly decreased the leakage and was able to restore the RPE barrier (Fig. 5D and 5E).

Effect of NMDAR Deletion in RPE cells on Hcy-induced CNV and retinal thickness

RPE flat mounts isolated from mouse retinas after one week of intravitreal injection of Hcy were prepared per our previously published method (9, 18, 24, 26) and stained with immunofluorescence stain for vascular marker using Isolectin-B4 (red) and NMDAR (green). Mounts are showing that Hcy injection induced choroidal neovascularization and activation of NMDAR which was more evident in the HHcy mice (*cbs*$^{+/-}$ mice and Hcy injected mice) compared to wild type control non-injected mice and *NMDAR*$^{R-/-}$ mice. Deletion of NMDAR in RPE cells was able to reduce the CNV induction and NMDAR activation by Hcy injection (Fig. 6A). OCT images and Insight® software were used for assessment of the thickness of different retinal layers in wild type and *NMDAR*$^{R-/-}$ mice after 72 hours of intravitreal injection of Hcy. The average thickness of each layer in a 300mm section of wild type mice and *NMDAR*$^{R-/-}$ mice retina were compared. Analysis of retinal thickness showing that RPE layer was significantly restored and choroid layer (CNV induction) was significantly decreased in Hcy-injected *NMDAR*$^{R-/-}$ mice compared to Hcy-injected wild type mice (Fig. 6B, C).

Discussion

The current study presents evidences suggest that activation of NMDAR as a possible mechanism of HHcy-induced BRB dysfunction, features of AMD and CNV induction. Our pervious findings showed that HHcy produced AMD like features in the RPE and induced CNV *in vivo* when was injected in mice eye and

in vitro in RPE cells treated with different concentrations of Hcy (9). Data presented in the current study 1) showed activation of NMDAR in RPE cells by HHcy *in vivo* and *in vitro*, 2) Confirmed the activation of NMDAR by Hcy at the level of RPE cells and that blocking of NMDAR attenuates Hcy-induced features of AMD, retinal hyperpermeability and development of CNV. 3) Tested blocking of NMDAR by pharmacological inhibition using MK801 and molecular inhibition using RPE NMDAR conditional knockout mouse that was created in our lab ($NMDAR^{R-/-}$).

The current study emphasizes the involvement of NMDAR in Hcy-induced outer BRB dysfunction, Hcy-induced features of AMD and CNV induction. AMD is the most common cause of blindness in elderly people (36). Generally, AMD is divided into two stages, early and late age-related maculopathy (ARM), according to the International Classification and Grading System (37). Advanced stage (late) AMD is further classified into two subtypes of AMD; non-neovascular (dry, atrophic) and neovascular (wet, exudative) types. Non-exudative AMD is characterized by gradual loss of RPE layer and thinning of the retina and only few preventative/therapeutic measures are currently available for the dry type (38). Conversely, exudative AMD is characterized by CNV and a subretinal neovascular fibrous tissue. CNV is responsible for 80% of AMD severe vision loss cases (39). Anti-VEGF therapy has demonstrated great benefit for the wet type, however issues, such as non-responses or the need for repeated injections continue to occur (40). The mechanisms of AMD progression are not completely understood. Accumulating evidence from many published clinical studies are in consistence with our results which revealed an associations between elevated plasma Hcy level and the risk AMD (6, 41) (42) predominantly the neurovascular (wet) AMD (38, 43). Furthermore, reported data from a case control study that was conducted in a tertiary eye care hospital with 32 diagnosed AMD patients supports our results which showed that HHcy was significantly associated with the wet AMD patients but not with the dry AMD patients(44).

Previously we reported a direct angiogenic effect of Hcy on human retinal endothelial cells (HREC) (11) and activation of NMDA receptors in retinal endothelial cells by Hcy (18). NMDAR activation was also reported to induce hyperpermeability by HHcy in retinal neurons and cerebral endothelial cells in several studies (16, 45-48). The study also demonstrated that Hcy level was significantly increased in the serum of neovascular AMD patients. This was associated with decreased Hcy clearance as indicated by decrease in CBS enzyme's level. Therefore, we suggested that HHcy as an important player in the pathogenesis of AMD. To explore the fact that HHcy is more involved in neovascular AMD, we tested the ability of Hcy to induce CNV after laser induction in wild type mice with/without intravitreal injection of Hcy. Our results showed that laser induction induced CNV in mice retina which was significantly more severe in Hcy-injected mice compared to non-injected mice. The current study confirmed our pervious finding both in vitro and in vivo. Our data showed that Hcy increased FITC-dextran leakage in RPE, fluorescein and albumin leakage as well as the development of CNV in mice eye when Hcy was injected intravitreal. Furthermore, our results showed that blocking NMDAR at the RPE level either by pharmacological or molecular inhibition was able to buffer the effect of HHcy on the barrier function both in vitro and in vivo.

Hypoxia plays a key role in retinal ischemia and neovascularization and it is the main stimulus for angiogenesis. Previously, we reported tissue hypoxia in the cbs mice retina (mice with HHcy) with upregulation of VEGF and development of neovascularization (10). Cellular responses to hypoxia are mediated by hypoxia-inducible transcription factors (HIFs) that are stabilized in hypoxia and prompt the up-regulates the activity of many genes involved in angiogenesis including VEGF (49)-(50, 51). HIF-1 is a nuclear protein which activates gene transcription in case of reduced oxygen tension. HIF-1 is a heterodimer composed of HIF-lα and HIF-1β subunits. HIF-1β is constitutively expressed while HIF-lα is induced and accumulates by hypoxia. HIF-1α, HIF-1 heterodimer increases the expression of angiogenesis and glycolysis genes. VEGF is the main angiogenic factor which is activated by HIF-1 to improve the hypoxic condition via stimulating vascular growth. This is consistent with the presented findings that HHcy activated HIF-1α and VEGF expression in the RPE cells and Ki67 in MCEC indicating its proliferation. Increased production of the proangiogenic factor VEGF from RPE cells plays the major role in CNV formation (52)-(53). Subsequently, proangiogenic factor VEGF leads to degradation of extracellular matrix via releasing inflammatory mediators from endothelial cells. VEGF is known to cause a breakdown of the BRB and increase retinal vascular permeability and leakage (54)-(55).

Moreover, to test the angiogenic effect of Hcy, we tested the effect of Hcy on RPE and MCEC cells. Our results showed that Hcy treatment significantly increased the protein levels of both HIF-lα and VEGF in ARPE-19 cell line and in primary RPE isolated from *cbs*$^{+/-}$ mice compared to control non treated ARPE-19 cells and wild type mice RPE. MCEC treated with Hcy showed activation of its proliferation indicated by upregulation of Ki67. These results proved that angiogenesis is a part of Hcy mechanism of BRB dysfunction and CNV induction.

We proposed that Hcy participates in the pathogenesis of AMD, induces CNV and angiogenesis via activation of NMDA receptor due to the similarity between Hcy and L-glutamate structure. In congruence, Hcy was reported to binds to NMDAR which is a glutamate receptor in neurons (15) and to activate NMDAR in cerebral endothelium resulting in disruption of tight junctions and blood brain barrier (BBB) dysfunction. Therefore, NMDAR could be a target for therapeutic intervention in HHcy (16)-(17). Additionally, several studies suggested that activation of NMDA receptors could be a possible mechanism of HHcy-induced retinal ganglion cell death (12) (56) (15). Recently, reported that hHcy induced-retinal endothelial cells dysfunction is mediated via activation of NMDAR signaling pathway (18).

The dramatic decline in cardiovascular mortality in the United States since 1950 may possibly be attributable in part to intended fortification of the food supply with vitamin B-6 and folic acid, apparently because of increased blood folate and decreased blood homocysteine, which is a well-known risk factor for cardiovascular diseases(57). Furthermore, combined vitamin-B6, B12 and folate were reported to exert a neuroprotective effects against hypoxia in mice brain (58).our future plans is aiming to test the effect of vitamins B12 and folic acid supplementation on Hcy-induced BRB dysfunction and CNV induction. However, the current study aimed to test the role of NMDAR in RPE cells in the pathogenesis of HHcy-induced AMD like features. First, we tested the expression of NMDA receptor in RPE cells. We assessed

the NMDA receptor expression in both primary RPE isolated from *cbs* mice (*cbs* $^{+/+}$ *and cbs* $^{+/-}$, mice with HHcy) and human retinal RPE cell line (ARPE-19). Our data showed that NMDAR is expressed in both cbs-RPE and human ARPE-19 cell line. Furthermore, cbs $^{+/-}$primary RPE cells showed higher expression of NMDAR than the wild type (*cbs* $^{+/+}$*)* RPE indicating activation of the NMDAR by Hcy. Moreover, Hcy treatment (100 μM) significantly increased NMDAR1 in ARPE-19 cells compared to untreated cells. These results confirmed possibility that Hcy participates in the pathogenesis of AMD via activation of NMDA receptor in RPE cells. Consistent with our hypothesis; the involvement of NMDAR activation in RPE was reported in many publications (21, 59) (60) and NMDAR blocker Memantine was reported to have a protective effect on the ARPE-19 cells [59].

Then, to prove our hypothesis *in vivo* we generated mice deficient in NMDAR in RPE cells (*NMDAR* $^{R-/-}$) and performed more experiments to tested if the deletion of NMDAR in RPE cells 1)-will protect the retina from the harmful effect of Hcy 2)-will preserve the BRB indicated by retinal vascular leakage 3)-will halt the progression of Hcy-induced CNV. For this purpose, living mice injected intravitreal with/without Hcy were exposed to FA and OCT examinations and albumin leakage assessment. FA and OCT results showed that knocking down the NMDAR in RPE cells decreased fluorescein leakage and CNV induction. Preservation of the BRB function was confirmed by measurement of albumin leakage after Hcy intravitreal injection of wild-type mice and *NMDAR* $^{R-/-}$ mice retinas. Blocking NMDAR at the RPE level significantly decreased albumin leakage compared to Hcy-injected wild type mice retinas. Furthermore, when mice were exposed to laser induction of CNV, knocking down the NMDAR in RPE cells protected the retina and showed less CNV induction than Hcy injected WT mice. This protective effect of knocking down the NMDAR in RPE cells was confirmed by measuring retinal thickness. The results showed that RPE layer was significantly restored while choroid layer (CNV induction) was significantly decreased in Hcy-injected *NMDAR* $^{R-/-}$ mice compared to Hcy-injected wild type mice. Therefore, these findings highlighted implication of NMDA receptor in Hcy-induced AMD like features.

In conclusion, the presented findings of the current study highlighted new molecular mechanisms for HHcy-induced RPE dysfunction. Indeed, our data from *in vivo* and *in vitro* experiments demonstrated NMDAR activation as underlying molecular target for Hcy in AMD retina. Unraveling these molecular targets help better understanding and shed the light on novel therapeutic approaches for HHcy-induced retinal damage and CNV induction in AMD patients.

Declarations

Ethics approval and consent to participate:

All experimental procedures were performed according to the Public Health Service Guide for the Care and Use of Laboratory Animals (Department of Health, Education, and Welfare publication, NIH 80-23) and Augusta University guidelines and followed the ARVO Statement for Use of Animals in Ophthalmic and Vision Research.

The patient's blood samples were provided by Dr. Margaret M. DeAngelis and Institutional Review Board (IRB) was approved by the University of Utah. Donor samples were collected, determined, managed and phenotyped as previously defined for the Utah protocol. This protocol was approved by the IRB (IRB 00052879) at the University of Utah and conforms to the tenets of the Declaration of Helsink.

Consent for publication: Not applicable.

Availability of data and materials: Western blot data was available as supplementary material. The rest of Data is available on reasonable request from corresponding author.

Competing interests: The authors declare that they have no competing interests.

Funding:

NEI grant award R01 EY029751-01–NEI00072 and NEI grant award R01 EY030054.

Authors' contributions: YS: the conception, design of the work, the acquisition, analysis and drafted the work; DK: the acquisition, analysis and interpretation of data; PR: the acquisition, analysis and interpretation of data; RM: the acquisition, analysis and interpretation of data; LO: collect the patient's blood samples; AS: collect the patient's blood samples; IK: collect the patient's blood samples; MD: provide the patient's blood samples; NS: provide the MCEC cells and revised the work ; MA: provide the OCT machine and revised the work; AT: the conception, design of the work, the analysis, interpretation of data and revised the work. All authors read and approved the final manuscript.

Acknowledgements: Not applicable.

References

1. Schmidt, K. G., Bergert, H., and Funk, R. H. Neurodegenerative diseases of the retina and potential for protection and recovery. *Current neuropharmacology*. 2008;**6**:164-178.
2. Wong, W. L., Su, X., Li, X., Cheung, C. M., Klein, R., Cheng, C. Y., and Wong, T. Y. Global prevalence of age-related macular degeneration and disease burden projection for 2020 and 2040: a systematic review and meta-analysis. *Lancet Glob Health*. 2014;**2**:e106-116.
3. Rein, D. B., Wittenborn, J. S., Zhang, X., Honeycutt, A. A., Lesesne, S. B., Saaddine, J., and Vision Health Cost-Effectiveness Study, G. Forecasting age-related macular degeneration through the year 2050: the potential impact of new treatments. *Arch Ophthalmol*. 2009;**127**:533-540.
4. DeAngelis, M. M., Owen, L. A., Morrison, M. A., Morgan, D. J., Li, M., Shakoor, A., Vitale, A., Iyengar, S., Stambolian, D., Kim, I. K., and Farrer, L. A. Genetics of age-related macular degeneration (AMD). *Hum Mol Genet*. 2017;**26**:R45-R50.
5. Obeid, R., Ninios, K., Loew, U., Gatzioufas, Z., Hoffmann, S., Seitz, B., Geisel, J., and Herrmann, W. Aqueous humor glycation marker and plasma homocysteine in macular degeneration. *Clinical chemistry and laboratory medicine*. 2013;**51**:657-663.

6. Kamburoglu, G., Gumus, K., Kadayifcilar, S., and Eldem, B. Plasma homocysteine, vitamin B12 and folate levels in age-related macular degeneration. *Graefes Arch Clin Exp Ophthalmol*. 2006;**244**:565-569.
7. Seddon, J. M., Gensler, G., Klein, M. L., and Milton, R. C. Evaluation of plasma homocysteine and risk of age-related macular degeneration. *American journal of ophthalmology.* 2006;**141**:201-203.
8. Nowak, M., Swietochowska, E., Wielkoszynski, T., Marek, B., Kos-Kudla, B., Szapska, B., Kajdaniuk, D., Glogowska-Szelag, J., Sieminska, L., Ostrowska, Z., Koziol, H., and Klimek, J. Homocysteine, vitamin B12, and folic acid in age-related macular degeneration. *European journal of ophthalmology*. 2005;**15**:764-767.
9. Ibrahim, A. S., Mander, S., Hussein, K. A., Elsherbiny, N. M., Smith, S. B., Al-Shabrawey, M., and Tawfik, A. Hyperhomocysteinemia disrupts retinal pigment epithelial structure and function with features of age-related macular degeneration. *Oncotarget*. 2016;**7**:8532-8545.
10. Tawfik, A., Markand, S., Al-Shabrawey, M., Mayo, J. N., Reynolds, J., Bearden, S. E., Ganapathy, V., and Smith, S. B. Alterations of retinal vasculature in cystathionine-beta-synthase heterozygous mice: a model of mild to moderate hyperhomocysteinemia. *Am J Pathol*. 2014;**184**:2573-2585.
11. Mohamed, R., Sharma, I., Ibrahim, A. S., Saleh, H., Elsherbiny, N. M., Fulzele, S., Elmasry, K., Smith, S. B., Al-Shabrawey, M., and Tawfik, A. Hyperhomocysteinemia Alters Retinal Endothelial Cells Barrier Function and Angiogenic Potential via Activation of Oxidative Stress. *Sci Rep.* 2017; **7**:11952.
12. Diederen, R. M., La Heij, E. C., Deutz, N. E., Kijlstra, A., Kessels, A. G., van Eijk, H. M., Liem, A. T., Dieudonne, S., and Hendrikse, F. Increased glutamate levels in the vitreous of patients with retinal detachment. *Experimental eye research.* 2006;**83**:45-50.
13. Ola, M. S., Hosoya, K., and LaNoue, K. F. Regulation of glutamate metabolism by hydrocortisone and branched chain keto acids in cultured rat retinal Muller cells (TR-MUL). *Neurochem Int*. 2011;**59**:656-663.
14. Yu, X. H., Zhang, H., Wang, Y. H., Liu, L. J., Teng, Y., and Liu, P. Time-dependent reduction of glutamine synthetase in retina of diabetic rats. *Exp Eye Res*. 2009;**89**:967-971.
15. Lipton, S. A., Kim, W. K., Choi, Y. B., Kumar, S., D'Emilia, D. M., Rayudu, P. V., Arnelle, D. R., and Stamler, J. S. Neurotoxicity associated with dual actions of homocysteine at the N-methyl-D-aspartate receptor. *Proc Natl Acad Sci U S A.* 1997;**94**:5923-5928.
16. Liu, X., Hunter, C., Weiss, H. R., and Chi, O. Z. Effects of blockade of ionotropic glutamate receptors on blood-brain barrier disruption in focal cerebral ischemia. *Neurol Sci*. 2010;**31**:699-703.
17. Andras, I. E., Deli, M. A., Veszelka, S., Hayashi, K., Hennig, B., and Toborek, M. The NMDA and AMPA/KA receptors are involved in glutamate-induced alterations of occludin expression and phosphorylation in brain endothelial cells. *Journal of cerebral blood flow and metabolism : official journal of the International Society of Cerebral Blood Flow and Metabolism.* 2007;**27**: 1431-1443.
18. Tawfik, A., Mohamed, R., Kira, D., Alhusban, S., and Al-Shabrawey, M. N-Methyl-D-aspartate receptor activation, novel mechanism of homocysteine-induced blood-retinal barrier dysfunction. *J Mol Med (Berl)*. 2020.

19. Lau, A., and Tymianski, M. Glutamate receptors, neurotoxicity and neurodegeneration. *Pflugers Archiv : European journal of physiology.* 2010;**460**:525-542.
20. Hardingham, G. E. Coupling of the NMDA receptor to neuroprotective and neurodestructive events. *Biochemical Society transactions*. 2009;**37**:1147-1160.
21. Uchida, N., Kiuchi, Y., Miyamoto, K., Uchida, J., Tobe, T., Tomita, M., Shioda, S., Nakai, Y., Koide, R., and Oguchi, K. Glutamate-stimulated proliferation of rat retinal pigment epithelial cells. *Eur J Pharmacol*. 1998;**343**:265-273.
22. Sawicki, A. [Calcium absorption in the digestive tract and calcium and phosphorus metabolism in postoperative hypoparathyroidism]. *Pol Arch Med Wewn.* 1986;**75**:417-423.
23. Henney, C. S. The specificity of the early immune response to dinitrophenylated human gamma-G-globulin. *Immunochemistry.* 1970;**7**:275-287.
24. Elmasry, K., Mohamed, R., Sharma, I., Elsherbiny, N. M., Liu, Y., Al-Shabrawey, M., and Tawfik, A. Epigenetic modifications in hyperhomocysteinemia: potential role in diabetic retinopathy and age-related macular degeneration. *Oncotarget*. 2018;**9**:12562-12590.
25. Tawfik, A., and Smith, S. B. Increased ER stress as a mechanism of retinal neurovasculopathy in mice with severe hyperhomocysteinemia. *Austin J Clin Ophthalmol*. 2014;**1**:1023.
26. Tawfik, A., Mohamed, R., Elsherbiny, N. M., DeAngelis, M. M., Bartoli, M., and Al-Shabrawey, M. Homocysteine: A Potential Biomarker for Diabetic Retinopathy. *J Clin Med.* 2019;**8.**
27. Elsherbiny, N. M., Sharma, I., Kira, D., Alhusban, S., Samra, Y. A., Jadeja, R., Martin, P., Al-Shabrawey, M., and Tawfik, A. Homocysteine Induces Inflammation in Retina and Brain. *Biomolecules.* 2020;**10.**
28. Nita, M., Grzybowski, A., Ascaso, F. J., and Huerva, V. Age-related macular degeneration in the aspect of chronic low-grade inflammation (pathophysiological parainflammation). *Mediators Inflamm*. 2014;**2014**:930671.
29. Elmasry K, Mohamed R, Sharma I, Elsherbiny N, Y, L., M, A.-S., and Tawfik A. Epigenetic modifications in hyperhomocysteinemia; potential role in diabetic retinopathy and age-related macular degeneration. *Oncotarget.* 2018;*https://doi.org/10.18632/oncotarget.24333*
30. Owen, L. A., Shakoor, A., Morgan, D. J., Hejazi, A. A., McEntire, M. W., Brown, J. J., Farrer, L. A., Kim, I., Vitale, A., and DeAngelis, M. M. The Utah Protocol for Postmortem Eye Phenotyping and Molecular Biochemical Analysis. *Invest Ophthalmol Vis Sci*. 2019;**60**:1204-1212.
31. Age-Related Eye Disease Study Research, G. The Age-Related Eye Disease Study system for classifying age-related macular degeneration from stereoscopic color fundus photographs: the Age-Related Eye Disease Study Report Number 6. *Am J Ophthalmol*. 2001;**132**:668-681.
32. Martin, P. M., Ananth, S., Cresci, G., Roon, P., Smith, S., and Ganapathy, V. Expression and localization of GPR109A (PUMA-G/HM74A) mRNA and protein in mammalian retinal pigment epithelium. *Molecular vision*. 2009;**15**:362-372.
33. Fei, P., Zaitoun, I., Farnoodian, M., Fisk, D. L., Wang, S., Sorenson, C. M., and Sheibani, N. Expression of thrombospondin-1 modulates the angioinflammatory phenotype of choroidal endothelial cells. *PLoS One*. 2014;**9**:e116423.

34. Murakami, T., Felinski, E. A., and Antonetti, D. A. Occludin phosphorylation and ubiquitination regulate tight junction trafficking and vascular endothelial growth factor-induced permeability. *J Biol Chem*. 2009;**284**:21036-21046.

35. Forooghian, F., Razavi, R., and Timms, L. Hypoxia-inducible factor expression in human RPE cells. *Br J Ophthalmol.* 2007;**91**:1406-1410.

36. Bird, A. C. Therapeutic targets in age-related macular disease. *The Journal of clinical investigation*. 2010;**120**:3033-3041.

37. Bird, A. C., Bressler, N. M., Bressler, S. B., Chisholm, I. H., Coscas, G., Davis, M. D., de Jong, P. T., Klaver, C. C., Klein, B. E., Klein, R., and et al. An international classification and grading system for age-related maculopathy and age-related macular degeneration. The International ARM Epidemiological Study Group. *Surv Ophthalmol*. 1995;**39**:367-374.

38. Chew, E. Y., Clemons, T. E., Agron, E., Sperduto, R. D., Sangiovanni, J. P., Kurinij, N., Davis, M. D., and Age-Related Eye Disease Study Research, G. Long-term effects of vitamins C and E, beta-carotene, and zinc on age-related macular degeneration: AREDS report no. 35. *Ophthalmology.* 2013;**120**:1604-1611 e1604.

39. Ferris, F. L., 3rd, Fine, S. L., and Hyman, L. Age-related macular degeneration and blindness due to neovascular maculopathy. *Archives of ophthalmology*. 1984;**102**:1640-1642.

40. Ding, X., Patel, M., and Chan, C. C. Molecular pathology of age-related macular degeneration. *Progress in retinal and eye research*. 2009;**28**:1-18.

41. Ates, O., Azizi, S., Alp, H. H., Kiziltunc, A., Beydemir, S., Cinici, E., Kocer, I., and Baykal, O. Decreased serum paraoxonase 1 activity and increased serum homocysteine and malondialdehyde levels in age-related macular degeneration. *Tohoku J Exp Med*. 2009;**217**:17-22.

42. Huang, P., Wang, F., Sah, B. K., Jiang, J., Ni, Z., Wang, J., and Sun, X. Homocysteine and the risk of age-related macular degeneration: a systematic review and meta-analysis. *Sci Rep*. 2015;**5**: 10585.

43. Javadzadeh, A., Ghorbanihaghjo, A., Bahreini, E., Rashtchizadeh, N., Argani, H., and Alizadeh, S. Plasma oxidized LDL and thiol-containing molecules in patients with exudative age-related macular degeneration. *Mol Vis*. 2010;**16**:2578-2584.

44. Ghosh, S., Saha, M., and Das, D. A study on plasma homocysteine level in age-related macular degeneration. *Nepal J Ophthalmol*. 2013;**5**:195-200.

45. Tawfik, A., Samra, Y. A., Elsherbiny, N. M., and Al-Shabrawey, M. Implication of Hyperhomocysteinemia in Blood Retinal Barrier (BRB) Dysfunction. *Biomolecules*. 2020;**10.**

46. Beard, R. S., Jr., Reynolds, J. J., and Bearden, S. E. Hyperhomocysteinemia increases permeability of the blood-brain barrier by NMDA receptor-dependent regulation of adherens and tight junctions. *Blood.* 2011;**118**:2007-2014.

47. Sharp, C. D., Hines, I., Houghton, J., Warren, A., Jackson, T. H. t., Jawahar, A., Nanda, A., Elrod, J. W., Long, A., Chi, A., Minagar, A., and Alexander, J. S. Glutamate causes a loss in human cerebral endothelial barrier integrity through activation of NMDA receptor. *Am J Physiol Heart Circ Physiol*. 2003;**285**:H2592-2598.

48. Kalani, A., Kamat, P. K., Tyagi, S. C., and Tyagi, N. Synergy of homocysteine, microRNA, and epigenetics: a novel therapeutic approach for stroke. *Mol Neurobiol*. 2013;**48**:157-168.
49. Semenza, G. L. Hypoxia-inducible factor 1: oxygen homeostasis and disease pathophysiology. *Trends Mol Med*. 2001;**7**:345-350.
50. Andre, H., Tunik, S., Aronsson, M., and Kvanta, A. Hypoxia-Inducible Factor-1alpha Is Associated With Sprouting Angiogenesis in the Murine Laser-Induced Choroidal Neovascularization Model. *Invest Ophthalmol Vis Sci*. 2015;**56**:6591-6604.
51. Mowat, F. M., Luhmann, U. F., Smith, A. J., Lange, C., Duran, Y., Harten, S., Shukla, D., Maxwell, P. H., Ali, R. R., and Bainbridge, J. W. HIF-1alpha and HIF-2alpha are differentially activated in distinct cell populations in retinal ischaemia. *PLoS One*. 2010;**5**:e11103.
52. Barchitta, M., and Maugeri, A. Association between Vascular Endothelial Growth Factor Polymorphisms and Age-Related Macular Degeneration: An Updated Meta-Analysis. *Dis Markers.* 2016;**2016**:8486406.
53. Kwak, N., Okamoto, N., Wood, J. M., and Campochiaro, P. A. VEGF is major stimulator in model of choroidal neovascularization. *Investigative ophthalmology & visual science*. 2000;**41**:3158-3164.
54. Aiello, L. P., Pierce, E. A., Foley, E. D., Takagi, H., Chen, H., Riddle, L., Ferrara, N., King, G. L., and Smith, L. E. Suppression of retinal neovascularization in vivo by inhibition of vascular endothelial growth factor (VEGF) using soluble VEGF-receptor chimeric proteins. *Proceedings of the National Academy of Sciences of the United States of America*. 1995;**92**:10457-10461.
55. Ozaki, H., Hayashi, H., Vinores, S. A., Moromizato, Y., Campochiaro, P. A., and Oshima, K. Intravitreal sustained release of VEGF causes retinal neovascularization in rabbits and breakdown of the blood-retinal barrier in rabbits and primates. *Experimental eye research.* 1997;**64**:505-517.
56. Ganapathy, P. S., Perry, R. L., Tawfik, A., Smith, R. M., Perry, E., Roon, P., Bozard, B. R., Ha, Y., and Smith, S. B. Homocysteine-mediated modulation of mitochondrial dynamics in retinal ganglion cells. *Invest Ophthalmol Vis Sci*. 2011;**52**:5551-5558.
57. McCully, K. S. Homocysteine, vitamins, and vascular disease prevention. *Am J Clin Nutr*. 2007;**86**: 1563S-1568S.
58. Yu, L., Chen, Y., Wang, W., Xiao, Z., and Hong, Y. Multi-Vitamin B Supplementation Reverses Hypoxia-Induced Tau Hyperphosphorylation and Improves Memory Function in Adult Mice. *J Alzheimers Dis*. 2016;**54**:297-306.
59. Garcia, S., Lopez, E., and Lopez-Colome, A. M. Glutamate accelerates RPE cell proliferation through ERK1/2 activation via distinct receptor-specific mechanisms. *J Cell Biochem.* 2008;**104**: 377-390.
60. Reigada, D., Lu, W., and Mitchell, C. H. Glutamate acts at NMDA receptors on fresh bovine and on cultured human retinal pigment epithelial cells to trigger release of ATP. *J Physiol.* 2006;**575**: 707-720.

Figures

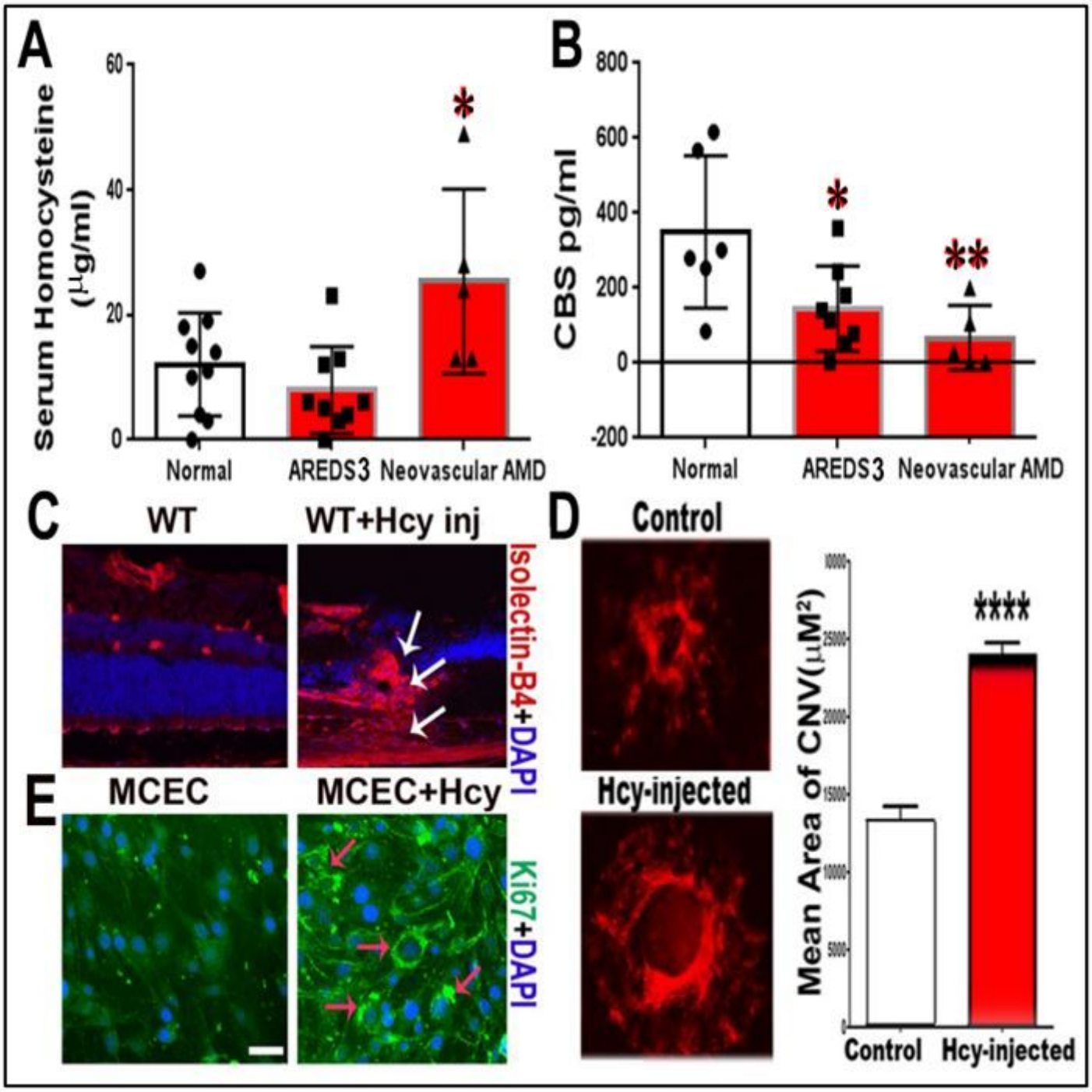

Figure 1

Homocysteine promotes angiogenesis and induces choroidal neovascularization (CNV). A) ELISA measurement of serum Hcy showing significant increase in patients with neovascular AMD. B) ELISA measurement of serum CBS enzyme showing significant decrease in patients with neovascular AMD. C) Intravitreal injection of Hcy in wild type mice induced choroidal neovascularization (CNV) as shown in retinal sections stained with isolectin-B4 (Arrows). D) Flat mount retina stained with isolectin-B4 showing that Hcy significantly increased the extent of laser-induced CNV in wild type mice. E) Immunofluorescence staining showing marked increase in the immunoreactivity of the proliferation

factor Ki67 in cultured mouse choroidal endothelial cells (green) by Hcy treatment. Calibration bar; 50 μm and *p < 0.05, **p < 0.01, and ***p < 0.001.

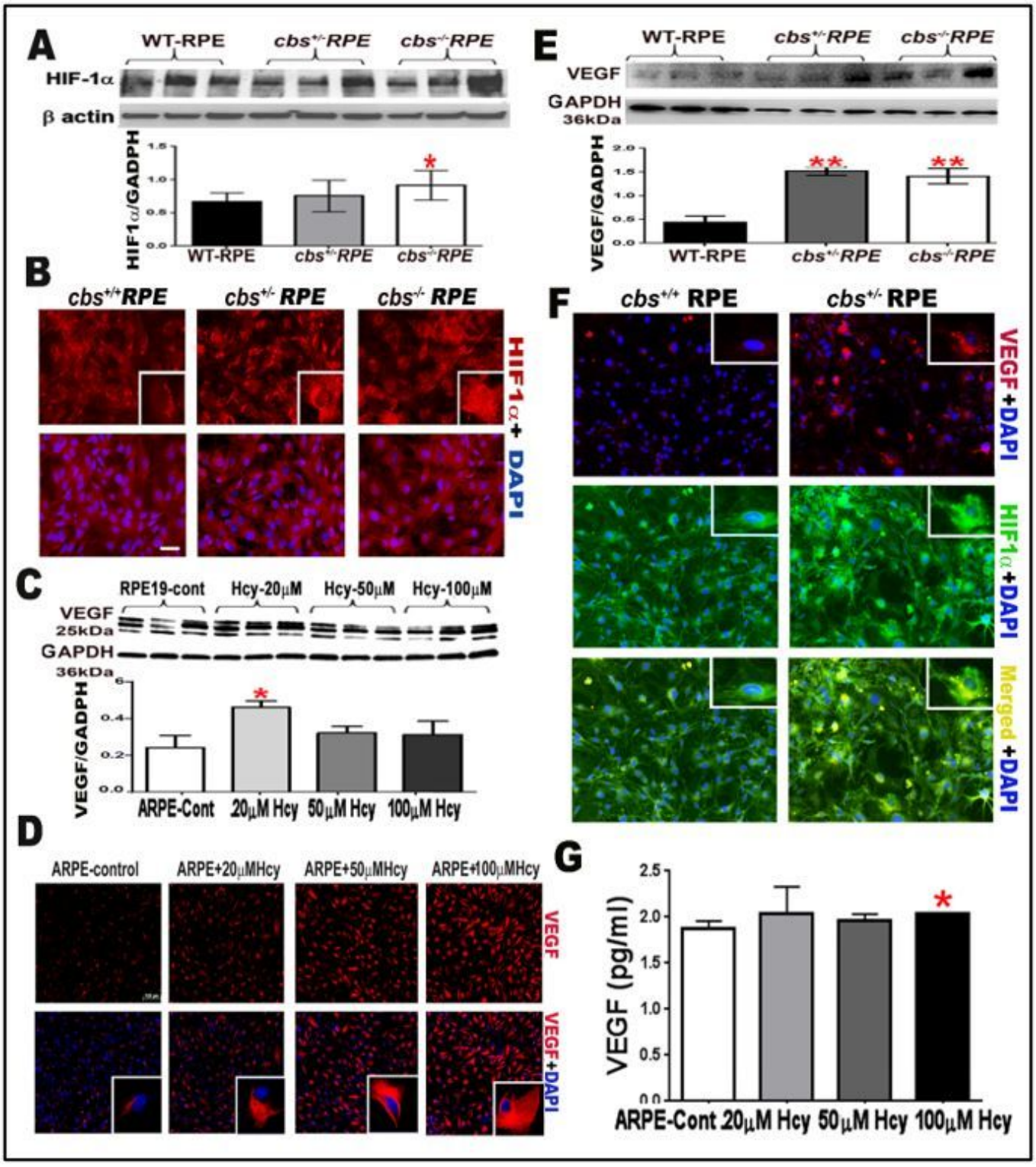

Figure 2

Homocysteine promotes angiogenic factors A) Western blotting of HIF-1α expression in primary RPE cells isolated from mice model of elevated Hcy (wild type cbs+/+ , cbs+/- and cbs-/-) showing significant increase in HIF-1α expression in mice with marked HHcy, ßactin was used as loading control B)

Immunofluorescence staining for HIF-1α (red) and nuclear staining (DAPI, blue) for primary RPE cells isolated from cbs+/+ cbs+/- and cbs-/- mice. C) Western blotting of VEGF expression in ARPE-19 treated with different concentration of Hcy (20, 50, and 100 μM representing mild/moderate and sever elevation of Hcy), GADPH was used as a loading control. D) Immunofluorescence staining for VEGF (red) and nuclear staining (DAPI, blue) for ARPE-19 treated with different concentration of Hcy (20, 50, and 100 μM). E) Western blotting of VEGF expression in primary RPE cells isolated from wild type cbs+/+ , cbs+/- and cbs-/- mice. GADPH was used as a loading control F) Immunofluorescence staining for VEGF (red), HIF-1α (green) and nuclear staining (DAPI, blue) for RPE cells isolated from cbs+/+, cbs+/- mice. G) ELISA evaluation of VEGF level in ARPE-19 treated with different concentration of Hcy (20, 50, and 100μM). Calibration bar; 50 μm, *$p<0.05$, **$p<0.01$.

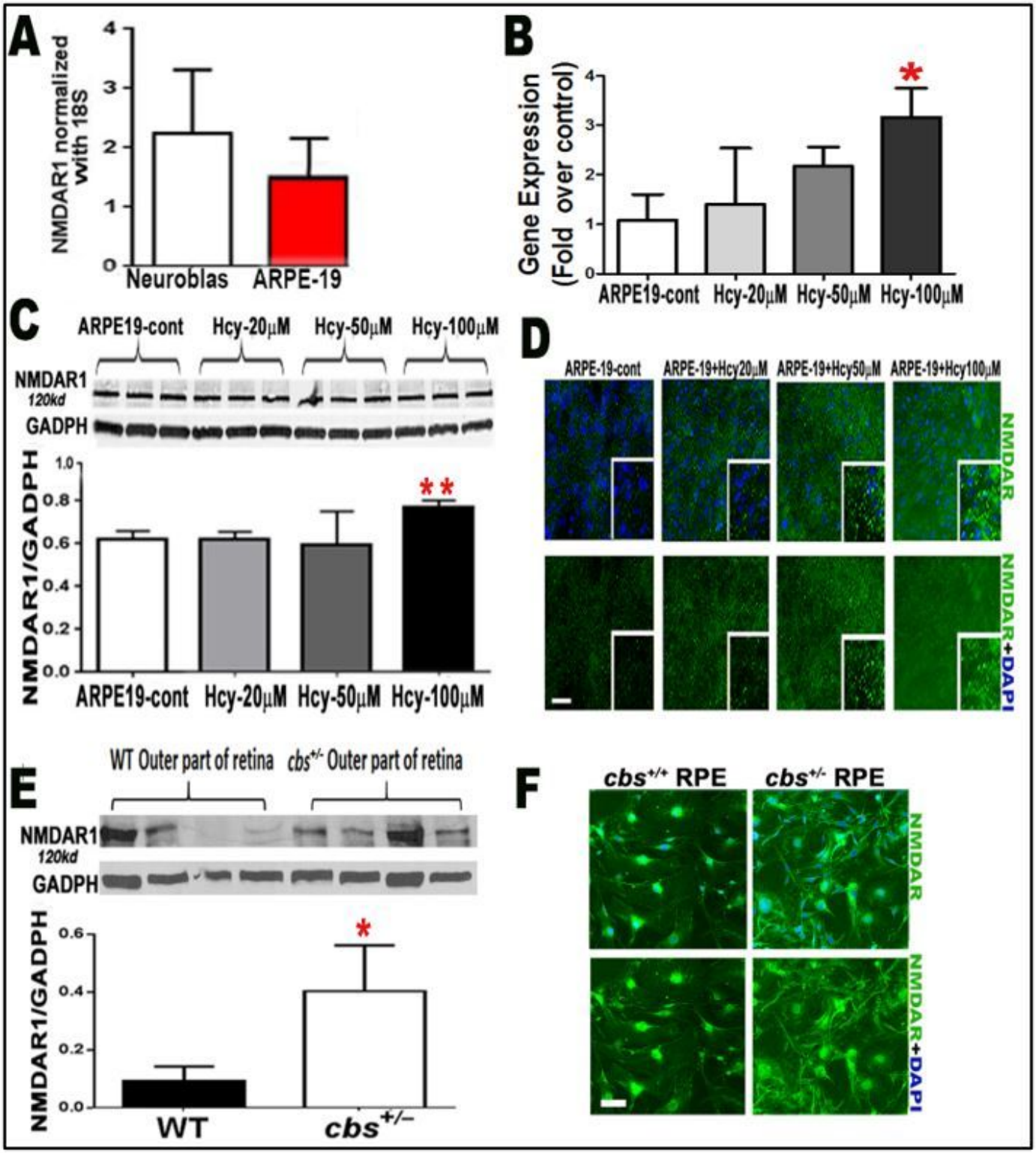

Figure 3

Evaluation of retinal epithelial cells (RPE) NMDAR expression in both in vivo and in vitro models of HHcy. A) RT-qPCR analysis showing the expression of NMDAR subunit NR1 in human RPE (ARPE-19) cell line compared to human neuroblastoma cells (ATCC CRL-2266) as a positive control. B) RT-qPCR analysis confirming NMDA receptor subunits NR1 (120 kD) in ARPE-19 cells and its activation by Hcy treatment (20 and 50μM) compared control untreated cells. C) Western blot analysis showing the expression of

NMDAR subunit NR1 in human RPE (ARPE-19) treated with different concentrations of Hcy (20, 50 and 100μM Hcy). GADPH was used as a loading control. D) IF analysis showing increased expression of NMDAR1 (green) in ARPE-19 treated with different concentrations of Hcy (20, 50 and 100μM Hcy). E) Western blot analysis showing the expression of NMDAR in the outer retina (containing mainly RPE cells) part of the WT mice and cbs+/- mice. GADPH was used as a loading control. F) IF analysis showing increased expression of NMDAR1 (green) in primary RPE cells isolated from cbs+/- mice. Calibration bar; 50 μm and *p < 0.05 and **p < 0.01.

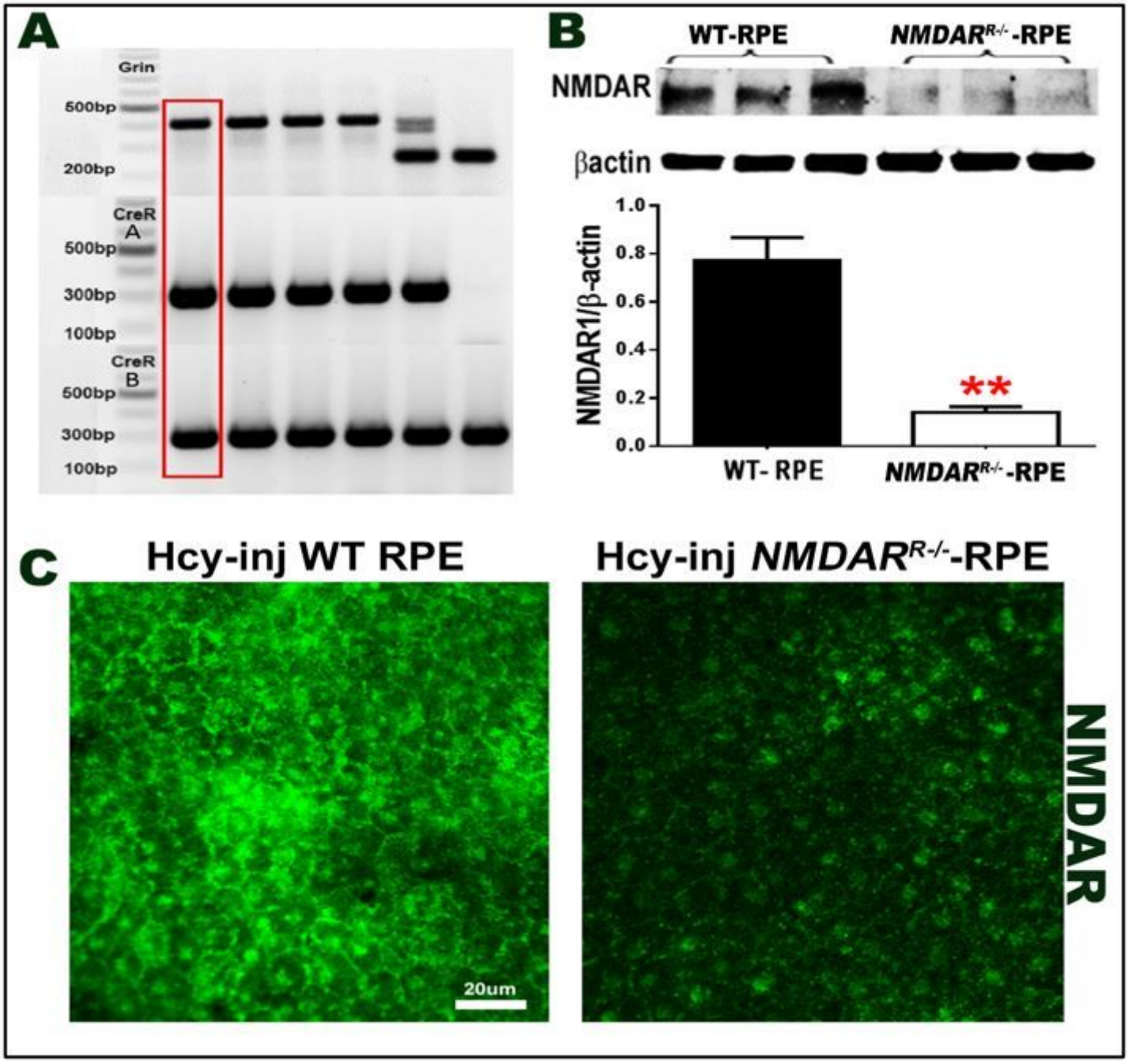

Figure 4

Mouse with genetic deletion of NMDAR (NMDARR-/-). Mouse deficient in NMDAR in the retinal epithelial cells (NMDARR-/-) was generated in our lab by backcrossing of B6.129S4-Grin1tm2Stl/J: (otherwise

known as: NR1flox, fNR1) with CreR mouse A) PCR, genotyping analysis. Grin genotyping results. (Grin+/+) has only one band ~ 400bp. (Grin+/-) has two bands ~ 400bp and 232bp. (Grin-/-), wildtype has a band at ~232bp. CreR genotyping results. CreR reactionA+ has band at 300bp and CreR reaction B+ has band at 300bp. The red labeled (NMDAr-/-R) = Grin+/+ CreR reaction A+/CreR reaction B+. B) Western blot analysis to confirm reduced expression of NMDAR in primary RPE cells isolated from wild type mice retina and primary RPE cells isolated from NMDARR-/- , which showed marked reduction in comparison to normal WT mice. ßactin was used as a loading control. C) Immunofluorescence expression of NMDAR (green) of RPE flat-mounts from control wild type and NMDARR-/- mice after intravitreal injection of Hcy which showed marked reduction of NMDAR expression in the RPE layer of the mouse retina of the NMDARR-/-mice compared to control. Calibration bar; 20 µm. *P < 0.05, and **p < 0.01.

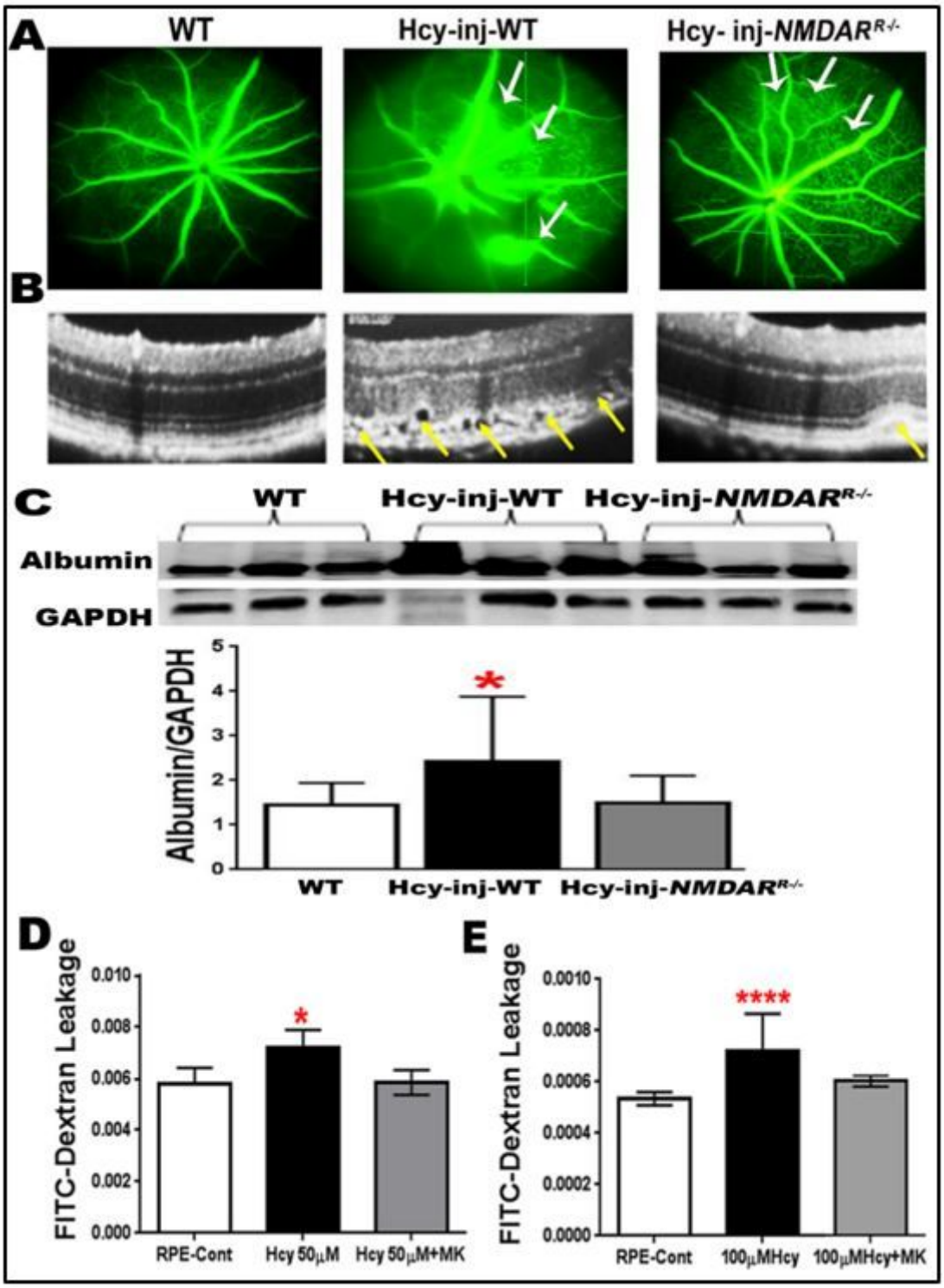

Figure 5

Knocking down the NMDAR in RPE cells (NMDAR R -/- mice) protects retina from Homocysteine induced Blood retinal barrier (BRB) dysfunction and choroidal neovascularization (CNV). C57BL6 mice with/without Hcy-thiolactone intravitreal injection or genetic inhibition of NMDAR (NMADRR-/-) were evaluated 72 hours after injection of Hcy by A) FA evaluation showing normal well-formed vessels in WT mouse; however, angiograms for Hcy injected mouse retinas show marked vascular leakage appears as diffused hyperfluorescence (white arrows), which was markedly reduced after knocking down NMDAR in

RPE (NMDARR-/-) mouse. B) OCT examination presenting normal appearance in the WT mice's retina, marked interruption of retinal morphology with hyporeflective subretinal lucency, focal hyper reflective spots, and choroidal neovascularization (yellow arrows) in Hcy injected mouse retinas. Knocking down NMDAR in RPE was able to reduce the retinal disruption, CNV and improved retinal structure after Hcy injection in NMDARR-/-mice (yellow arrows), (n = 6 mice/group). C) Reduced vascular leakage after knocking down NMDAR in RPE was confirmed by measuring the albumin leakage in the retinas by western blotting, which was significantly increased in the Hcy-injected mice eye, but reduced to normal level in Hcy-injected NMDARR-/-mice *p<0.05. Improvement of retinal morphology and CNV induction was further evaluated by assessment of retinal thickness in Hcy injected mice. . D) FITC dextran flux through RPE monolayer, which revealed significant increase in FITC dextran leakage in 50 μM Hcy-treated RPE cells and decreased by MK801 treatment. E) FITC dextran flux through RPE monolayer, which revealed significant increase in FITC dextran leakage in 100 μM Hcy-treated RPE cells and decreased by MK801 treatment. *P < 0.05, **p < 0.01 and ***p < 0.001,

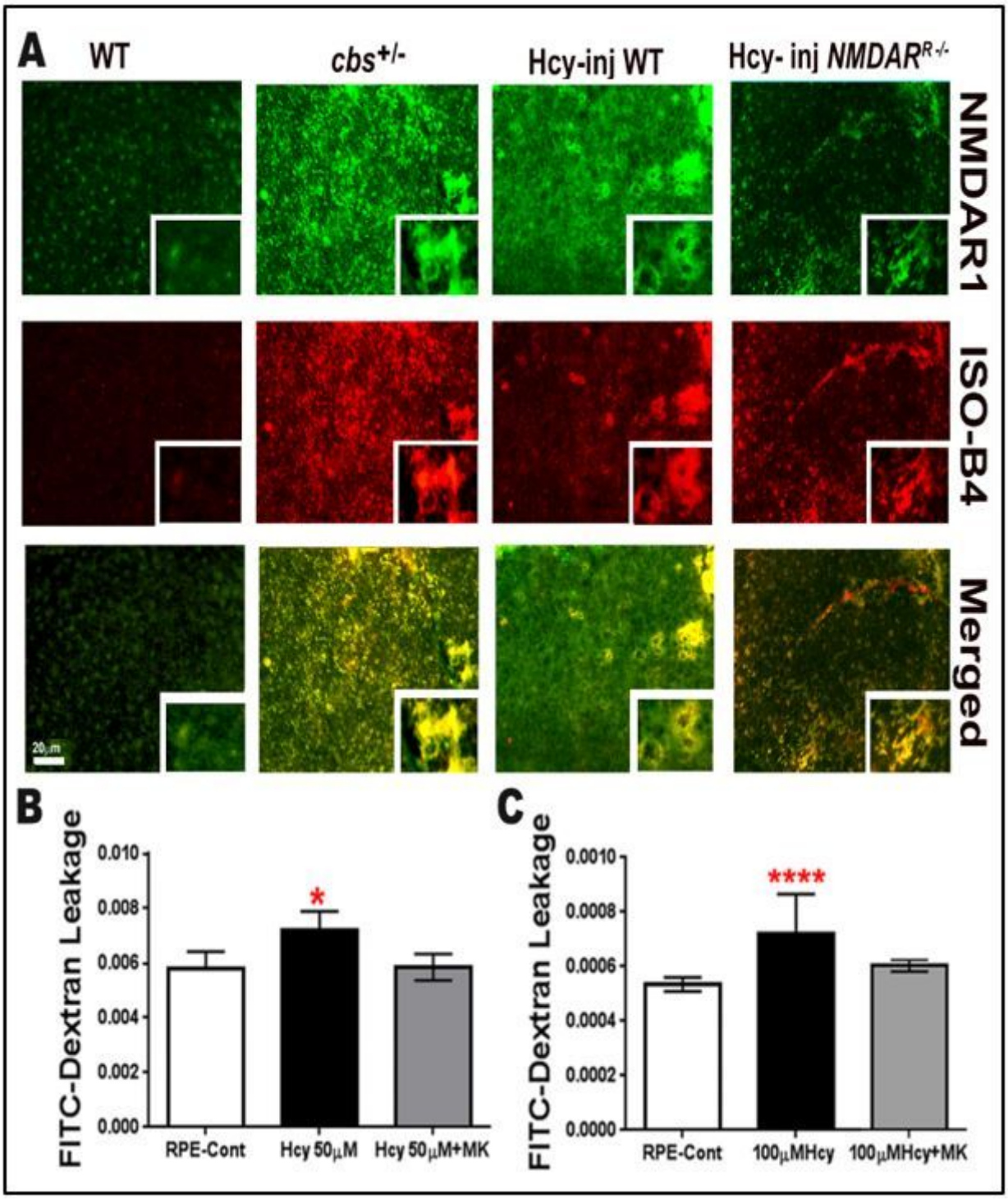

Figure 6

Deletion of NMDAR in RPE cells decreased Hcy induced CNV in retinal flat mounts A) immunofluorescence staining for RPE flat mounts isolated from mouse retinas after one week of intravitreal injection of Hcy in WT and NMDARR -/- compared to WT- control non-injected mice and mice with HHcy (cbs+/-) stained with vascular marker using Isolectin-B4 (red) and NMDAR1 (green). Hcy injection induced choroidal neovascularization and activation of NMDAR which was more evident in both mice models of HHcy (cbs+/- mice and Hcy injected-WT mice), while Knocking down NMDAR in

(NMDARR -/-) was able to reduce the CNV induction and NMDAR activation by Hcy injection. B) OCT images and Insight® software were used for assessment of the thickness of different retinal layers in wild type and NMDARR-/-mice after 72 hours of intravitreal injection of Hcy. C) Analysis of retinal thickness from WT-mice and NMDARR-/- mice injected with Hcy, shows improved RPE layer and decreased CNV size in NMDARR-/-mice. Mice number/6/group. Calibration bar; 20 μm *p<0.05, **p<0.01.

Supplementary Files

This is a list of supplementary files associated with this preprint. Click to download.

- WBRawdata.pdf